Revista de la Academia Colombiana de Ciencias Exactas, Físicas y Naturales. 2024
doi: https://doi.org/10.18257/raccefyn.2651

Physical Sciences

Original article

Ca_2TiFeO_6 ordered perovskite: A comprehensive study of its structure and magnetic attributes

Perovskita ordenada Ca_2TiFeO_6: un estudio exhaustivo de su estructura y atributos magnéticos

Laura Vanessa Parra-Mesa[1,*], Carlos A. Parra-Vargas[2], Indry M. Saavedra-Gaona[2], David A. Landínez-Téllez[1,3], Jairo Roa-Rojas[1,3]

[1] Grupo de Física de Nuevos Materiales, Departamento de Física, Universidad Nacional de Colombia, Bogotá DC, Colombia
[2] Grupo de Física de Materiales, Escuela de Física, Universidad Pedagógica y Tecnológica de Colombia, Tunja, Colombia
[3] Grupo de Estudios de Materiales GEMA, Departamento de Física, Universidad Nacional de Colombia, Bogotá D.C., Colombia

Abstract

The use of materials in contemporary technology heavily relies on their nanostructural, physical, and chemical attributes. The specific domain within technology referred to as spintronics, encompasses the realm of spin transport electronics. Spintronics delves into the electron spin, its inherent magnetic moment and fundamental charge, and the manipulation of these intrinsic characteristics to develop solid-state devices. In metallic systems, spintronics encloses phenomena like spin-charge coupling, which includes ferro- and ferrimagnetic materials, giant and colossal magnetoresistive materials, and metallic spins. Among the most versatile materials in the evidence of exotic properties, one of the most representative families is the so-called perovskites, widely studied in recent years including their properties in solar cell technology. Here, we present some crystallographic, compositional, morphological, optical, and magnetic attributes of the Ca_2TiFeO_6 double perovskite material, synthesized by the standard solid-state reaction method from high-purity precursor oxides. Rietveld refinement of experimental X-ray diffraction data revealed that this material crystallizes in a monoclinic perovskite-type structure with alternating ordering of Ti-Fe cations along the three crystallographic axes. The strongly granular surface character of the Ca_2TiFeO_6 materials was observed in the images from a scanning electron microscope; the electron X-ray energy dispersive spectra revealed a close match of sample composition to that expected from their chemical formula. The diffuse reflectance spectrum showed the semiconductor feature of the material with a 1.02 eV bandgap. The magnetic characterization in the 50 K < T < 335 K regime and the applied fields up to 1 kOe showed the ferromagnetic response of the material over the entire temperature range measured. These properties are promising in the spintronics industry for devices where the same material serves to process, record, read, and erase information as in the spin transistors.

Keywords: Double perovskite; Structure; Ferromagnetism; Semiconductor; Spintronics.

Resumen

La utilización de materiales en la tecnología contemporánea depende en gran medida de sus atributos nanoestructurales, físicos y químicos. El ámbito tecnológico específico de la espintrónica abarca la electrónica de transporte de espín. La espintrónica estudia a profundidad el espín electrónico, su momento magnético inherente, la carga fundamental y la manipulación de estas características intrínsecas para el desarrollo de dispositivos de estado sólido. En los sistemas metálicos, la espintrónica explora fenómenos como el acoplamiento espín-carga, incluidos los materiales ferro y ferrimagnéticos, los materiales magnetorresistivos gigantes y colosales, y los espines metálicos. Entre los materiales más versátiles en la evidencia de propiedades exóticas, una de las familias más representativas es la de las perovskitas, cuyas propiedades han sido ampliamente estudiadas en los últimos años en el campo de la tecnología de células solares. Presentamos aquí los atributos

Citation: Parra-Mesa LV, *et al.* Ca_2TiFeO_6 ordered perovskite: A comprehensive study of its structure and magnetic attributes. Revista de la Academia Colombiana de Ciencias Exactas, Físicas y Naturales. 2024 Ago 20. doi: https://doi.org/10.18257/raccefyn.2651

Editor: Rafael González Hernández

***Corresponding autor:**
Laura Vanessa Parra Mesa;
lparrame@unal.edu.co

Received: May 22, 2024
Accepted: July 31, 2024
Published on line: August 20, 2024

Revista de la Academia Colombiana de Ciencias Exactas, Físicas y Naturales. 2024
doi: https://doi.org/10.18257/raccefyn.2651

cristalográficos, composicionales, morfológicos, ópticos y magnéticos del material perovskita doble Ca_2TiFeO_6, sintetizados mediante el método estándar de reacción en estado sólido a partir de óxidos precursores de gran pureza. El refinamiento Rietveld de los datos experimentales de difracción de rayos X reveló que este material cristaliza en una estructura monoclínica de tipo perovskita con ordenación alternante de los cationes Ti-Fe a lo largo de los tres ejes cristalográficos. La naturaleza marcadamente granular de la superficie de los materiales Ca_2TiFeO_6 se observó mediante imágenes obtenidas en un microscopio electrónico de barrido y los espectros de dispersión de energía de rayos X electrónicos revelaron una estrecha correspondencia de la composición de las muestras con la esperada a partir de su fórmula química. El espectro de reflectancia difusa reveló la característica semiconductora del material con una banda prohibida de 1,02 eV. La caracterización magnética en el régimen de 50 K < T < 335 K y en campos aplicados de hasta 1 kOe evidenció la respuesta ferromagnética del material en todo el rango de temperatura medido. Estas propiedades generan expectativas tecnológicas en la industria espintrónica para la producción de dispositivos en los cuales un mismo material se utilice en el procesamiento y las operaciones de grabación, lectura y borrado de información como sucede en los transistores de espín.

Palabras clave: Perovskita doble; Estructura; Ferromagnetismo; Semiconductor; Espintrónica.

Introduction

Perovskites are an important basis for recent progress in solid-state physics, chemistry, and materials science. Perovskite-type oxides are characterized by the general form ABO_3, where A stands for an alkali earth metal lanthanide or semimetal of radius greater than B, B is usually a transition metal, and O is oxygen. These materials have been used in applications ranging from semiconductors, ferroelectrics, and superconductors to colossal magnetoresistive materials (**Kieslich *et al.***, 2014) used in the fabrication of nanomaterials (**Mao *et al.***, 2010) and high entropy composites (**Jiang *et al.***, 2017). Perovskites allow a wide spectrum of cations with different oxidation states in their structure (**Eng *et al.***, 2003) giving rise to a variety of compounds (**Bhalla *et al.,*** 2000) with a remarkable diversity of physical properties (**Cavichini, *et al.,*** 2018). Perovskites allow a wide spectrum of cations with different oxidation states in their structure (**Eng *et al.***, 2003) giving rise to a variety of compounds (**Bhalla *et al.***, 2000) with a remarkable diversity of physical properties (**Cavichini *et al.***, 2018). Perovskites adopt the ABO3 structure and also more complex forms such as the A2BB'O6- and AA'BB'O6-type double perovskites (**Lufaso & Woodward**, 2001), and other more complex ones (**Roa-Rojas *et al.***, 2022) with A and B sites occupied by two cations. These configurations indicate where cation inclusion occurs and their arrangement influences the material properties. Inclusion in A (less common than cation ordering in B) occurs in two different crystallographic sites, A and A', a configuration where the structural features limit the symmetries of complex perovskites, as cations in A favor a layered crystalline ordering (**King & Woodward**, 2010) endowing the material with magnetic and electrical properties (**Cuervo-Farfán *et al.***, 2018) and modifying its optical (**Deluque-Toro *et al.,*** 2023) and dielectric (**Jaramillo-Palacio *et al.,*** 2021) characteristics.

A family of double perovskite-type materials, with few studies given their difficulty of synthesis but promising physical properties, is based on calcium titanate with the inclusion of magnetic atoms to form the compound Ca_2TiMO_6, where M represents a magnetic cation. Ca_2TiMnO_6 was reported as an antiferromagnetic at Néel temperature 15.3 K with dielectric losses at room temperature that crystallized in a tetragonal structure belonging to space group I4/m (#87) (**Ochoa Burgos *et al.***, 2012). On the other hand, $CaTi_{0.5}Cr_{0.5}O_3$, reported as Ca_2TiCrO_6, is a simple $CaTiO_3$ perovskite substituted in 50% Cr at the Ti sites whose crystallization occurs in an orthorhombic structure (space group Pbnm, #62). Its main characteristic is the strongly frequency-dependent colossal dielectric character at room temperature (**Tan *et al.,*** 2013). When M=Fe, the $CaTi_{1-y}Fe_yO_{3-\delta}$ material adopts a thin film form with suggested cubic phase crystallization (space group Pm3m, #221) and band gap 3.4 eV semiconductor-type response. There are no reports on the magnetic nature of the material (**Yildirim *et al.***, 2022).

Here we aimed to examine the structural, morphological, optical, and magnetic properties of the Ca_2TiFeO_6 material to determine its multifunctional features and potential applicability in spintronic devices simultaneously combining the functions of magnetically stored information processing, erasing, writing, and reading.

Experimental procedures

We produced samples of the Ca_2TiFeO_6 material using the solid-state reaction ceramic method. The starting point was Sigma-Aldrich CaO, TiO_2, and Fe_3O_4 oxides with 99.99% purity dried at 120ºC and ground in an agate mortar for 3 h, which were then pressed into pellets and calcined at 800ºC for 48 h. After a 30 minute-maceration, the final sintering process was carried out at 1000ºC for 48 hours. For the structural characterization, we obtained diffraction patterns in a PANalytical X'pert-Pro diffractometer with $\lambda_{CuK\alpha}$=1.540598 Å radiation in the Bragg-Brentano configuration and a 0.001º step during 5 s. We used Rietveld refinement with the GSAS-II code for data analysis (**Toby & Von Dreele**, 2013). We obtained scanning electron microscope (SEM) images from a Vega 3 TESCAN using secondary and backscattered electron detectors. Using a Bruker detector coupled to the microscope we obtained X-ray energy dispersive spectra (EDS) for the semi-quantitative compositional analysis. For the optical characterization, we used a VARIAN Cary 5000 UV-vis-NIR spectrophotometer, and the magnetic response was measured with a VSM in a VersaLab Quantum Design equipment in the range from 50 K to 335 K for magnetic susceptibility following the Zero Field Cooling (ZFC) and Field Cooled (FC) recipes and magnetization curves as a function of the external fields up to ±1000 Oe.

Results and discussion

The Rietveld analysis of the experimental X-ray diffraction (XRD) data is shown in **figure 1.** We found a good correspondence between the experimental pattern (blue symbols) and the theoretical one (green line).

In **table 1**, we present the structural parameters resulting from the refinement: a characteristic monoclinic structure belonging to the space group $P2_1/n$ (#14), very similar to the orthorhombic structure of the Pnma space group (#62) typical of simple perovskites, except that in the monoclinic, one of the angles of the unit cell axes was slightly deviated from 90º. The main feature is that Ti and Fe cations form a salt rock-like superstructure arranged intercalary along the three crystallographic axes. **Table 1** also shows Wyckoff's positions (c, d, and e) that relate to the lattice points where the symmetry groups of each unit cell point become conjugate subgroups of the space group $P2_1/n$ (**Parthé *et al.***, 1993). These letters represent an encoding type for the atomic positions in the cell appearing always in alphabetical order (**Wondratschek**, 2006) while the numbers accompanying them determine the equivalent points per unit cell referred to as Wyckoff position multiplicity.

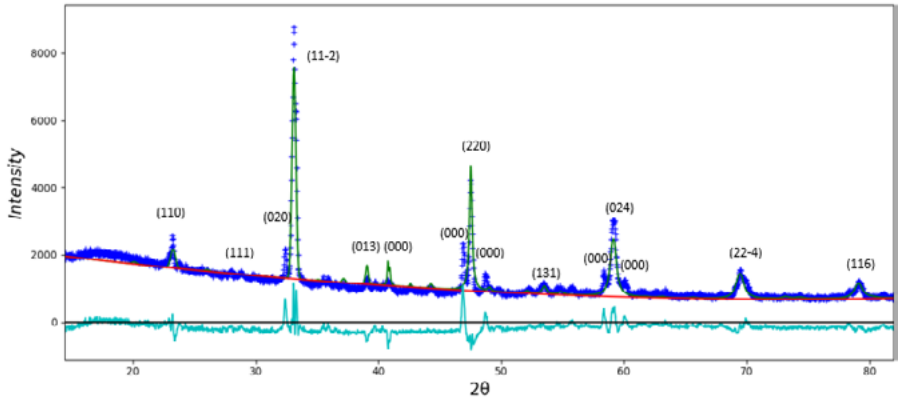

Figure 1. Diffraction pattern refined by Rietveld analysis for the material Ca_2TiFeO_6

Revista de la Academia Colombiana de Ciencias Exactas, Físicas y Naturales. 2024
doi: https://doi.org/10.18257/raccefyn.2651

Table 1. Structural parameters of Ca_2TiFeO_6 obtained from Rietveld refinement of the experimental XRD data

Lattice parameter (Å)	Atom	Wyckoff site	Atomic coordinates (±0.0001)		
			x	***y***	***z***
a=5.39833(2)	Ca	4e	0.5082	0.5272	0.2498
b=5.42707(1)	Ti	2c	0.0000	0.5000	0.0000
c=7.65120(2)	Fe	2d	0.5000	0.0000	0.0000
	O_1	4e	0.2188	0.2148	-0.0338
α= γ=90°	O_2	4e	0.2865	0.7199	-0.0339
β=90.061(1)o	O_3	4e	0.4323	-0.0087	0.2474
Refinement reliability parameters			$\chi^2 = 13.627$, $R_{exp} = 7.43$ %, $R_p = 11.08$ %, $R_{wp} = 10.16$%		

The distorted nature of the crystal cell for the Ca_2TiFeO_6 double perovskite-type material is shown in **table 1**. The positions outside the expected equilibrium sites of the anions in the cell provided the first indication of the distortional character of the TiO_6 and FeO_6 octahedra. Second, the evidence of octahedral tinting arose from the differences between the interatomic distances of the Ti and Fe cations concerning each of the O_1, O_2, and O_3 anions. The presence of Ti-O-Fe bond angles away from 180° and of ρ and η angles different from zero degrees corroborate the distorted feature of the structure. Third, the structural distortion was evidenced by the tolerance factor, defined as

$$\tau = \frac{r_{Ca}+r_O}{\sqrt{2}(\frac{r_{Ti}+r_{Fe}}{2}+r_O)}, \quad (1)$$

where r_{Ca}, r_{Ti}, and r_{Fe} are the ionic radii of the Ca, Ti, and Fe cations and r_O represents the ionic radius of oxygen. The ionic radii of the cations also influenced the octahedral distortions (**Woodward**, 1997). In their octahedral coordination, the ionic radius of Ti^{4+} is 0.605 Å and that of Fe^{4+} is 0.585 Å. The electrical (**Aleksandrov**, 1978) or magnetic **(Lufaso & Woodward**, 2004) character of the cations and their interaction with neighboring cations also contributed to the occurrence of distortions. The tolerance factor obtained was τ=0.9210, representing an 8% deviation of the unit cell from the perfectly cubic structure, for which τ=1 would be expected **(Landínez-Téllez *et al.***, 2014). In perovskite-type materials, octahedral tilts are well described by Glazer's notation (**Glazer**, 1972), whereby the Ca_2TiFeO_6 structure is denoted $a^-b^+a^-$. The superscript (-) represents an out-of-phase tilt while (+) represents an in-phase tilt, so in the Ca_2TiFeO_6 material, the octahedra rotate in phase along the crystallographic *b* axis and out of phase along the *a* and *c* axes.

The surface morphology of the samples is exemplified in **figure 2a** at 10 kx magnification. A formation of primary structures of strongly diffused irregular grains is shown. The agglomerates thus formed, interconnected with each other, evidencing a high porosity in the material. The small grains in diffusion had average dimensions of 653.8 nm (**Figure 2b**), while the clusters can reach micrometer sizes. The boundaries between agglomerates appeared irregular, blurring with those of neighboring clusters. On the other hand, pores occurred in the form of small dark regions and depressions in the surface topography of the sample. Clusters are portions of compact material formed by grains joined by "necks" through which intergranular diffusion takes place as the result of the high temperature of the thermal processes applied during the sintering of the samples. In **figure 2a**, the regions closest to the surface became bright because, due to the non-conducting nature of the Ca_2TiFeO_6 material, they were electrically charged when hit by the electron beam of the microscope.

We made a semi-quantitative estimate of the composition of the material through the characteristic X-ray detector of the microscope electron beam interactions with the surface of the sample, where the transitions between electronic orbitals emit radiation allowing an energy dispersion spectrum (**Figure 3**). Firstly, the EDS data of the spectrum suggested the absence of chemical elements other than those expected from the stoichiometric formula Ca_2TiFeO_6, so only those included in the solid-state reaction during the synthesis process appeared. Secondly, it was clear from the spectrum that the dominant intensities corresponded to K_α and K_β energy transitions of Ca, Ti, Fe, and oxygen K_α. As expected, the L_α transitions of Ca, Ti, and Fe were less intense and occurred at lower energy values. By deconvolution of the spectrum curve, it was possible to quantify the percentage proportion of each of the constituent atoms of the material. The values obtained were 97% in agreement with those expected from the stoichiometry Ca_2TiFeO_6, with 28.6%-Ca, 17.1%-Ti, 20.0%-Fe, and 34.3%-O.

After determining the structural and compositional characteristics of the material, we studied the properties that guarantee its applicability in modern technology. First, we characterized the optical response of the material using diffuse reflectance spectroscopy as shown in **figure 4a**, where the percentage of reflectance as a function of wavelength is represented. Three anomalies can be seen in the spectrum, as well as a discontinuity

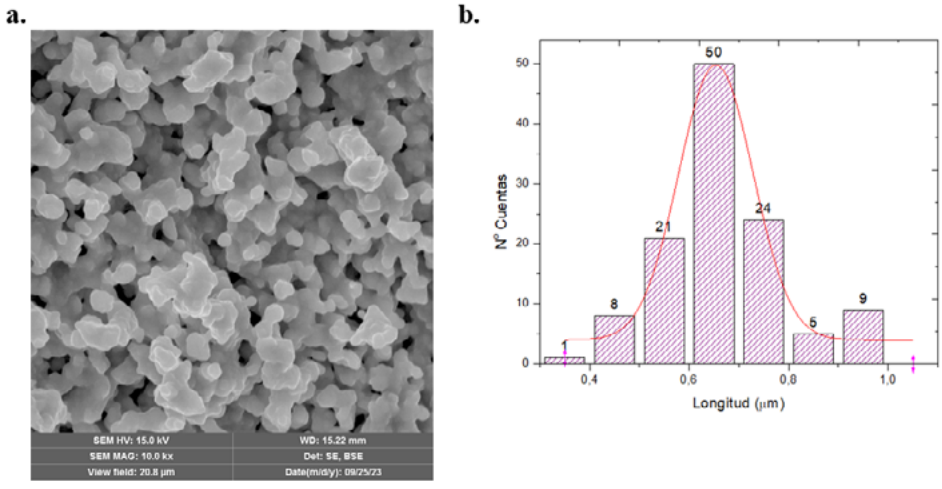

Figure 2. a. Surface microscopy image of a Ca_2TiFeO_6 double perovskite sample. **b.** Distribution of grain size in doble perovskite Ca_2TiFeO_6

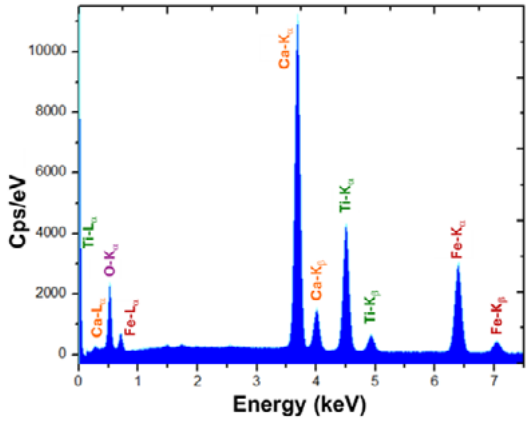

Figure 3. Surface grain energy dispersion spectrum for the Ca_2TiFeO_6 material

Revista de la Academia Colombiana de Ciencias Exactas, Físicas y Naturales. 2024
doi: https://doi.org/10.18257/raccefyn.2651

at λ=799 nm due to the change of lamp during the measuring process. These behavioral deviations in the spectrum are related to three vibrational modes observed by UV-vis of the eight that complete the irreducible representation for the double perovskite family (**Cuervo-Farfán *et al.***, 2017). The remaining five vibrational modes were observable by Raman spectroscopy (**Sorescu *et al.***, 2011) taking place at the Ti-O and Fe-O bonds of the octahedral coordination and the Ca-O bonds of the cuboctahedral coordination in the unit cell.

To obtain the value of an eventual optical bandgap, we performed a Kubelka-Munk-type analysis of the experimental data (**Kubelka & Munk**, 1931). As shown in **Figure 4b**, this analysis was done by modifying the Tauc equation for thick samples (**Kumar *et al.***, 1999) to finally obtain an E_g=1.02±0.02 eV bandgap, characteristic of semiconductor materials, such as $SnSe_2$ (**Mohebbi *et al.***, 2024).

Although Fe^{4+} in octahedral coordination does not exhibit orbital splitting due to the crystal field, there is evidence of its contribution to ferromagnetic (**Hayashi *et al.***, 2011) and antiferromagnetic (**Golubeva *et al.***, 2009) ordering in perovskites. For this reason, we measured the magnetic susceptibility as a function of temperature following the ZFC and FC procedures under an H=200 Oe field strength in the thermal regime 50 < T < 335 K. The result (**Figure 5**) was that at the highest temperature measured (T=335 K), there was a finite susceptibility value possibly indicating a magnetic ordering characteristic whose criticality occurs at higher temperatures.

Another interesting feature in the curve has to do with the irreversible response in ZFC and FC procedures denoting magnetic disorder effects associated with the microstructural randomness of the material. Finally, it is evident that from the beginning of the magnetization process at high temperatures up to T=335 K, the susceptibility increased by

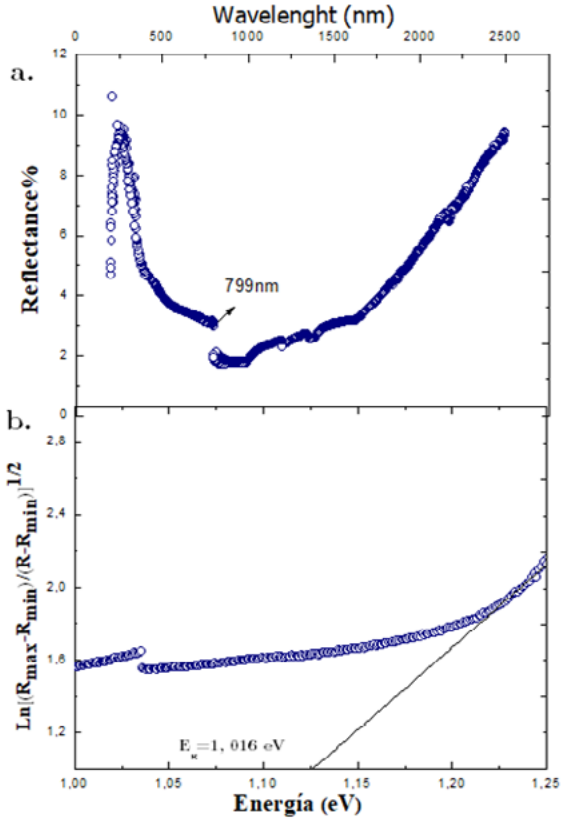

Figure 4. a) Diffuse reflectance spectrum and **b)** Kubelka-Munk analysis for obtaining the bandgap in the Ca_2TiFeO_6 samples

81.8% while in the 50 K < T < 335 K regime it increased by 18.2%. This shows that close to room temperatures and in the presence of a 100 Oe low field, the material presented magnetic ordering but still not all its domains had oriented to reach saturation, which can be achieved under the application of higher fields or lower temperatures.

To examine these effects more exhaustively, we did magnetization measurements as a function of the applied field (**Figure 6**). The curves revealed a hysteretic characteristic and although there was an increase in the coercive field with decreasing temperatures, the values were typical of soft ferromagnetic materials, which may have applicability in devices designed for reading and recording information on magnetic media. Additionally, the remanent magnetization also increased slightly with decreasing temperatures.

On the other hand, we observed that not only the coercive field and the remanent magnetization increased with decreasing temperatures but also the absolute value of the magnetization. This has to do with the observations already discussed above concerning the susceptibility curve as a function of temperature (**Figure 5**), where it is clear that

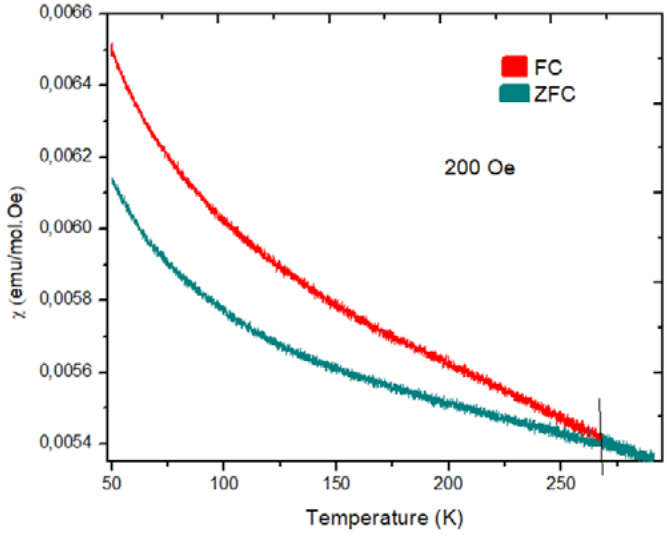

Figure 5. Susceptibility as a function of temperature measured in Ca_2TiFeO_6 samples

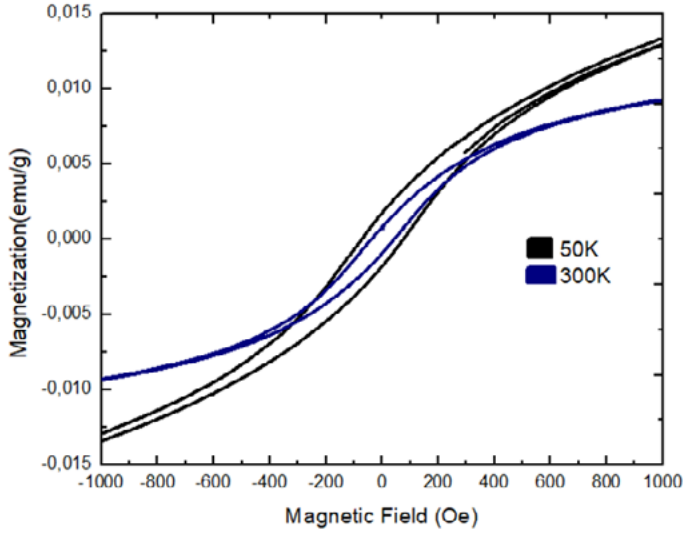

Figure 6. Magnetization as a function of the magnetic field measured in Ca_2TiFeO_6 samples

Revista de la Academia Colombiana de Ciencias Exactas, Físicas y Naturales. 2024
doi: https://doi.org/10.18257/raccefyn.2651

at lower temperatures the magnetic moment is higher due to the orientation of a greater number of magnetic domains in response to the application of the external field. Due to the ferromagnetic nature of Ca_2TiFeO_6 in the measurement regime, the occurrence of a Curie temperature above 335 K is expected.

Conclusions

We synthesized the material Ca_2TiFeO_6 by solid reaction. The Rietveld analysis of experimental X-ray diffraction data allowed us to establish that the material crystallized in a monoclinic perovskite-type structure (space group $P2_1/n$, #14) with Ti and Fe cations ordering along the crystallographic axes and forming a superstructure characteristic of double perovskites. We observed grains of submicrometer dimensions forming agglomerates of micrometer sizes in SEM images. Compositional analysis through EDS experiments corroborated the stoichiometry of the perovskite-type oxide Ca_2TiFeO_6. The optical characterization suggested the semiconductor character of the material with a 1.02 eV bandgap. Susceptibility measurements as a function of temperature and hysteresis curves allowed us to establish that the material behaved as a soft ferromagnet at Curie temperature higher than 335 K. The coexistence of semiconducting and ferromagnetic responses in the same crystallographic phase allowed us to classify the material as multifunctional with potential applicability in the design of spintronic devices such as spin transistors.

Acknowledgments

Our study was partially supported by the Dirección de Investigación y Extensión (DIEB) at the National University of Colombia (Hermes Code 57456).

Author contributions

LVPM synthesized the samples and performed the structural, morphological, and compositional characterizations. CAPV and IMSG performed the magnetic measurements. DALT coordinated the structural and morphological analyses. JRR proposed and directed the project, coordinated the work team, interpreted and correlated the experimental and theoretical results, analyzed the interaction mechanisms, and wrote the paper.

Conflicts of interest

The authors declare that there is no conflict of interest of any kind regarding the publication of the results of our research work.

References

Aleksandrov, K.S. (1978). Mechanisms of the ferroelectric and structural phase transitions. Structural distortions in perovskites. Ferroelectrics, *20,* 61-67.

Bhalla, A.S., Guo, R., Roy, R. (2000). The perovskite structure - A review of its role in ceramic science and technology. *Materials Research Innovations, 4*(1), 3-26.

Cavichini, A. S., Orlando, M. T., Depianti, J. B., Passamai Jr, J. L., Damay, F., Porcher, F., Granado, E. (2018). Exotic magnetism and spin-orbit-assisted Mott insulating state in a 3d-5d double perovskite. *Physical Review B, 97*(5), 054431.

Cuervo-Farfán, J. A., Aljure-García, D. M., Cardona, R., Arbey-Rodríguez, J., Landínez-Téllez, D. A., Roa-Rojas, J. (2017). Structure, ferromagnetic, dielectric and electronic features of the LaBiFe2O6 Material. *Journal of Low Temperature Physics, 186*, 295-315.

Cuervo-Farfán, J.A., Parra-Vargas, C.A., Viana, D.S.F., Milton, F.P., García, D., Landínez-Téllez, D.A., Roa-Rojas, J. (2018). Structural, magnetic, dielectric and optical properties of the Eu2Bi2Fe4O12 bismuth-based low-temperature biferroic. *Journal of Materials Science: Materials in Electronics, 29,* 20942-20951.

Deluque-Toro, C.E., Vergara, V.E., Gil-Rebaza, A.V., Landínez-Téllez, D. A., Roa-Rojas, J. (2023). Ground state structural, lattice dynamic, thermodynamic and optical properties of the Ba2CaMoO6 ordered perovskite. *Physica B: Condensed Matter, 666*, 415132.

Eng, H.W., Barnes, P.W., Auer, B.M., Woodward, P.M. (2003). Investigations of the electronic structure of d0 transition metal oxides belonging to the perovskite family. *Journal of Solid State Chemistry, 175*(1), 94-109.

Glazer, A.M. (1972). The classification of tilted octahedra in perovskites. *Acta Crystallographica B*, 28, 3384-3392.

Golubeva, O.Y., Semenov, V. G., Volodin, V.S., Gusarov, V.V. (2009). Structural stabilization of Fe4+ Ions in perovskite-like phases based on the BiFeO3-SrFeO y system. *Glass Physics and Chemistry, 35*, 313-319.

Hayashi, N., Yamamoto, T., Kageyama, H., Nishi, M., Watanabe, Y., Kawakami, T., Matsushita, Y., Fujimori, A., Takano, M. (2011). BaFeO3: A Ferromagnetic Iron Oxide. Angewandte Chemie International Edition, *50*, 12547-12550.

Jaramillo-Palacio, J.A., Muñoz-Pulido, K.A., Arbey-Rodríguez, J., Landínez-Téllez, D.A., Roa-Rojas, J. (2021). Electric, magnetic and microstructural features of the La2CoFeO6 lanthanide ferrocobaltite obtained by the modified Pechini route. *Journal of Advanced Dielectrics, 11*(03), 2140003.

Jiang, S., Hu, T., Gild, J., Zhou, N., Nie, J., Qin, M., Harrington, T., Veccio, K., Luo, J. (2017). A new class of high-entropy perovskite oxides. *Scripta Materialia, 142,* 116-120.

Kieslich, G., Sun, S., Cheetham, A.K. (2014). Solid-state principles applied to organic–inorganic perovskites: New tricks for an old dog. *Chemical Science, 5*(12), 4712-4715.

King, G. & Woodward, P.M. (2010). Cation ordering in perovskites. *Journal of Materials Chemitry A., 20*(28), 5785-5796.

Kubelka, P., Munk, F. (1931). An article on optics of paint layers. Z. *Technical Physics, 12*, 593.

Kumar, V., Sharma, S. K., Sharma, T. P.,Singh, V. (1999). Band gap determination in thick films from reflectance measurements. *Optical Materials, 12*, 115.

Landínez-Téllez, D.A., Martínez-Buitrago, D., Cardona C., R., Barrera, E. W., Roa-Rojas, J. (2014). Crystalline structure, magnetic response and electronic properties of RE2MgTiO6 (RE = Dy, Gd) double perovskites. *Journal of Molecular Structure, 1067*, 205-209.

Lufaso, M.W. & Woodward, P.M. (2001). Prediction of the crystal structures of perovskites using the software program SPuDS. *Acta Crystallographica Section B, 57*(6), 725-738.

Lufaso, M.W. & Woodward, P.M. (2004). Jahn–Teller distortions, cation ordering and octahedral tilting in perovskites. *Acta Crystallographica B, 60*, 10-20.

Mao, Y., Zhou, H., Wong, S. S. (2010). Synthesis, Properties, and Applications of Perovskite-Phase Metal Oxide Nanostructures Properties of Perovskite Systems. *Matererial Matters, 5*(2), 50.

Mohebbi, E., Pavoni, E., Pierantoni, L., Stipa, P., Zampa, G.M., Laudadio, E., Mencarelli, D. (2024). Band gap and THz optical adsorption of SnSe and SnSe2 nanosheets on graphene: Negative dielectric constant of SnSe. *Results in Physics, 57*, 107415.

Ochoa-Burgos, R., Martínez, D., Parra-Vargas, C. A., Landínez-Téllez, D. A., Vera-López, E., Sarmiento-Santos, A., Roa-Rojas, J. (2012). Magnetic and ferroelectric response of Ca2TiMnO6 manganite-like perovskite. *Revista Mexicana de Física S, 58*(2), 44–46.

Parthé, E., Gelato, L., Chabot, B., Penzo, M., Cenzual, K., Gladyshevskii, R. (1993). TYPIX Standardized and crystal chemical characterization of inorganic structure types. In: *Gmelein Handbook of Inorganic and Organometallic Chemistry, 8th ed*. Springer.

Roa-Rojas, J., Cuervo-Farfán, J. A., Deluque-Toro, C. E., Landínez-Téllez, D. A., Parra-Vargas, C. A. (2022). Rare-earth ferrobismuthites: ferromagnetic ceramic semiconductors with applicability in spintronic devices. *Revista de la Academia Colombiana de Ciencias Exactas, Físicas y Naturales, 9*, 628-645.

Sorescu, M., Xu, T., Hannan, A. (2011). Initial stage growth mechanism of LaFeO3 perovskite through magnetomechanical ball-milling of lanthanum and iron oxides. *American Journal of Materials Science, 1*, 57.

Tan, Y.-Q., Meng, Y., Yong-Mei, H. (2013). Structure and colossal dielectric permittivity of Ca2TiCrO6 ceramics. *Journal of Physics D: Applied Physics, 46,* 015303.

Toby, B.H., Von Dreele, R B. (2013). GSAS-II: the genesis of a modern open-source all-purpose crystallography software package. *Journal of Applied Crystallography, 46*, 544-549.

Wondratschek, W. (2006). International Tables for Crystallography, *Vol. A,* Chapter 8.3, 732-740. Springer, Dordrecht.

Woodward, P.M. (1997). Octahedral Tilting in Perovskites. I. Geometrical Considerations. *Acta Crystalographica B, 53*, 32-43.

Yildirim, C., Devoize, F., Geffroy, P.-M., Dumas-Bouchiat, F., Bouclé, J., Vedraine, S. (2022). Electrical and Optical Properties of CaTi1-yFeyO3-δ Perovskite Films as Interlayers for Optoelectronic Applications. *Materials, 15*, 6533.